한국해양환경공학회지
Journal of the Korean Society
for Marine Environmental Engineering
Vol. 10, No. 1. pp. 29-43, February 2007

생태계 모델에 의한 총허용오염부하량 산정을 통한 연안해역의 수질관리

이대인[1,†] · 김종규[2]
[1]전남대학교 수산과학연구소
[2]전남대학교 해양기술학부

Estimation of Total Allowable Pollutant Loads Using Eco-hydrodynamic Modeling for Water Quality Management on the Southern Coast of Korea

Dae-In Lee[1,†] and Jong-Kyu Kim[2]
[1]*The Fisheries Science Institute, Chonnam National University, Dundeok-dong, Yeosu, Jeollanam-do 550-749, Republic of Korea*
[2]*Faculty of Marine Technology, Chonnam National University, Dundeok-dong, Yeosu, Jeollanam-do 550-749, Republic of Korea*

요 약

한국 남해의 연안역(진해만에서 부산연안)에 있어서 효율적인 수질관리를 위해서, 3차원 생태-유체역학 모델을 적용하여 하계 수질을 예측하고, 목표 수질회복을 위한 오염부하 삭감량을 산정하였다. 현재의 오염부하량 조건하에서 연안해역의 수질(화학적 산소요구량과 영양염류 농도 등)은 설정된 해양환경수질기준을 초과하였고, 또한 부영양화 상태에 있기 때문에 유입하는 오염부하량의 저감이 필요하였다. 이러한 배경하에서, 모델이 적용되어 보정과 검증과정을 통해 연구해역의 유동장과 수질 분포를 유사하게 모의하였다. 시나리오 분석결과, 진해만 해역은 Chl-*a* 10 μg l^{-1}와 COD 3 mg l^{-1} 이하를 동시에 만족하기 위해서는 육상 점오염원으로부터 90% 정도의 오염물질 저감뿐만 아니라, 장기간 오염물질의 유입으로 인한 베이스 농도 자체가 높아서 이를 저감하기 위한 퇴적물로부터 용출되는 질소와 인도 약 70% 정도 삭감해야 하는 것으로 나타났다. 낙동강 하구해역은 Chl-*a* 10 μg l^{-1}와 COD 2 mg l^{-1} 이하를 만족하기 위해서는 낙동강 자체의 유입부하량을 약 80% 정도 저감해야 하며, 낙동강 하구해역을 제외한 부산 연안역은 Chl-*a* 10 μg l^{-1}와 COD 1 mg l^{-1} 이하를 만족하기 위해서는 유입부하의 70% 정도의 삭감이 이루어져야 하는 것으로 예측되었다. 연구해역의 수질이 공간적으로 차이가 있으나 대체적으로 상당히 오염된 상황이라 이러한 삭감량은 매우 커서 현실적으로 단기간에 달성하기는 어려울 것이다. 그러므로 장기적인 관점에서 지속적인 노력 즉, 해역으로 유입하는 미처리된 오염물질 차단, 수처리시설의 확충과 제거 능력 향상 및 오염된 퇴적물 정화 등이 필요하다.

Abstract – For effective management of water quality on the southern coast of Korea, a three-dimensional eco-hydrodynamic model is used to predict water quality in summer and to estimate the reduction rate in pollutant loads that would be required to restore water quality. Under the current environmental conditions, in particular, pollutant loadings to the study area were very high, chemical oxygen demand (COD) exceeded seawater quality criteria to comply with current legislation, and water quality was in a eutrophic condition. Therefore, we estimated reduction rates of current pollutant loads by modeling. The model reproduced reasonably the flow field and water quality of the study area. If the terrestrial COD, inorganic nitrogen and phosphorus loads were reduced by 90%, the water quality criteria of Region A were still not satisfied. However, when the nutrient loads from polluted sediment and land were each reduced by 70% simultaneously, COD and Chl-*a* were restored. When we reduced the input COD and nutrient loads from the Nakdong River by 80%, Chl-*a* and COD of Region B decreased below 10 μg l^{-1} and 2 mg l^{-1}, respectively. The water quality criteria of Region C were satisfied when we reduced the terrestrial COD and nutrient loads by 70%. Total allowable loadings of COD and inorganic nutrients in each region were determined by multiplying the reduction rates by current pollutant loads.

†Corresponding author: standby89@chonnam.ac.kr

Estimated high reduction rates, although difficult to achieve at the present time under the prevailing environmental conditions, suggest that water pollution is very severe in this study area, and pollutant loads must be reduced within total allowable loads by continuous and long-term management. To achieve the reduction in pollutant loads, sustainable countermeasures are necessary, including the expansion of sewage and wastewater facilities, polluted sediment control and limited land use.

Keywords: water quality management(수질관리), eco-hydrodynamic model(생태-유체역학 모델), pollutant loads(오염부하량), water quality criteria(수질기준), total allowable loadings(총허용오염부하량), the southern coast of Korea(한국 남해)

1. INTRODUCTION

Total allowable pollutant load is a similar concept to Total Maximum Daily Load (TMDL). TMDL is the maximum amount of pollutant that a water body can receive and still meet water quality standards, and an allocation of that amount to the pollutant's sources (USEPA [1997]). Government sets up water quality criteria for drinking water supply, contact recreation (swimming) and aquatic life support.

There is interaction between terrestrial and marine environments in coastal areas, as a result of human activities and the characteristics of the seas themselves. Chinhae Bay, which is located on the southeastern coast of Korea, is a semi-enclosed bay and one of the most heavily polluted coastal areas in this part of Korea. This bay has been used extensively in the past for mariculture, including the production of oysters, mussels and ark shells due to its favorable environmental conditions (Region A in Fig. 1). The coastal area of Busan, which is the second largest city in Korea and has about 4 million residents, has been used for beaches, port construction and mariculture grounds (Region C in Fig. 1). It includes the estuary of Nakdong River, one of Korea's four major river systems (Region B in Fig. 1). Recently, with deterioration of water and sediment quality due to increased sewage and wastewater inputs, artificial development and self-pollution from intensive aquaculture, shellfish productivity has decreased. In addition, water pollution including the occurrence of red tides, bottom water anoxia and toxic materials has frequently been observed (Hwang *et al.* [1999]; KORDI [1995]; MOE [1991]; NFRDI [1997]). For these reasons, the Korean government has designated these regions as special management areas for coastal pollution and has been conducting monitoring activities (Lee [1998]; MOMAF [2002]).

The Ministry of Maritime Affairs and Fisheries (MOMAF),

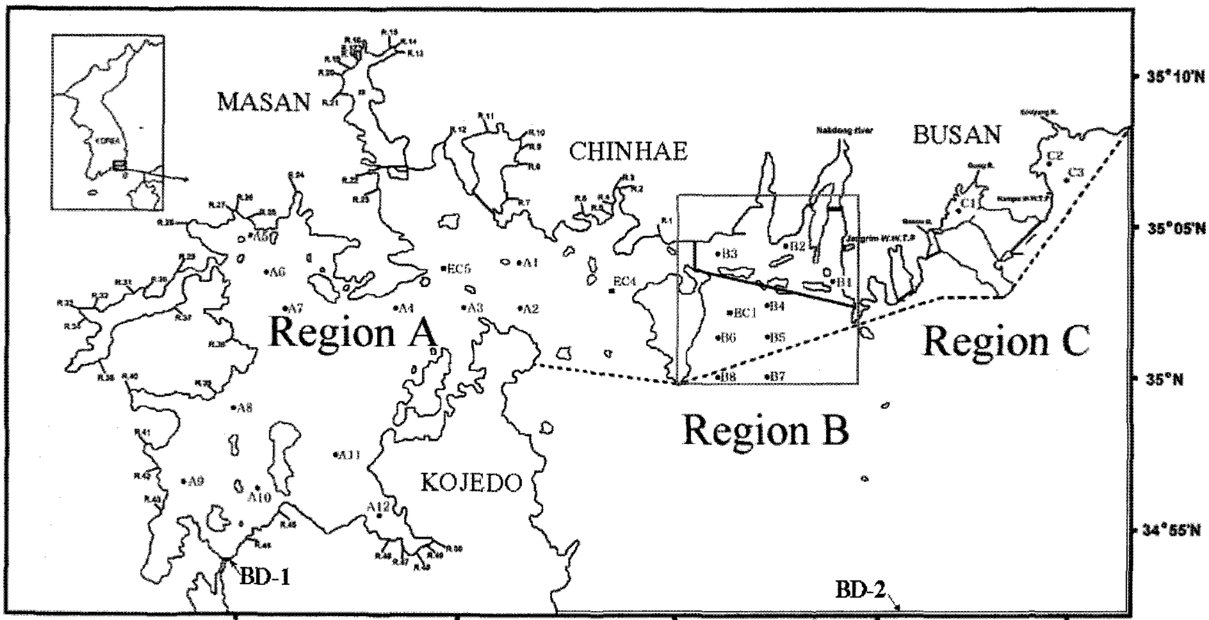

Fig. 1. Observation stations in the study area on the southern coast of Korea (Region A: Chinhae Bay, Region B: estuary of the Nakdong River, Region C: coastal seas of Busan).

which is responsible for the management of the coastal environment in Korea, has defined three grades of seawater quality. Grade I, with less than 1 mg l^{-1} chemical oxygen demand (COD) and more than 7.5 mg l^{-1} dissolved oxygen (DO), is suitable for mariculture and swimming. Grade II, with less than 2 mg l^{-1} COD and more than 5 mg l^{-1} DO, is suitable for leisure activities except swimming and mariculture for some aquatic species except Grade I species. Grade III, with less than 4 mg l^{-1} COD and more than 2 mg l^{-1} DO, is the water quality for harbor and industrial use.

As a result of increased and continuous pollutant loading, the observed summer water quality of the study area by NFRDI (National Fisheries Research & Development Institute) has been seriously degraded (Fig. 2). In Region A, the semi-enclosed inner bay, contamination levels are high; Chlorophyll-*a* (Chl-*a*), which indicates a standing crop of phytoplankton, exceeds the eutrophication index of 10 μg l^{-1} (National Academy of Science [1972]), and chemical oxygen demand (COD) exceeds seawater quality Grade II (below 2 mg l^{-1}), which is the current legal limit. Recently, the values of COD and Chl-*a* have decreased somewhat, but still remain high. In contrast, inputs of inorganic nitrogen and phosphorus have increased. Therefore, it is important to restore Chl-*a* and COD levels in this area to below 10 μg l^{-1} and 3 mg l^{-1}, respectively. Region B is a coastal estuary that is greatly impacted by freshwater discharge from the Nakdong River. Currently, the water quality in downstream reaches of the Nakdong River has seriously deteriorated (Lee & Park [2002]). Dissolved inorganic nitrogen (DIN) and dissolved inorganic phosphorus (DIP) are much higher in Region B than in the other two regions, owing to inputs of polluted freshwater through the estuary barrage. Chl-*a*, however, is lower in Region B than in Region A because of the influence of physical advection and diffusion, but red tides can occur, as they did in 1999, if the water column is stable. Apart from some inner areas, COD has been considered legally as being seawater quality Grade II. However, seawater quality is currently Grade III. The contamination level of Region C is less than that of the other two regions. COD, however, exceeds seawater quality Grade I because of increased input of inorganic matter, which is not removed in the water treatment process; Chl-*a* is also increasing. Therefore, water quality management of the study areas is very important for the effective and sustainable use of aquatic resources.

Although water quality in coastal zones can be determined by various factors, the effects of terrestrial pollution sources greatly predominate. That is, the physical and biogeochemical

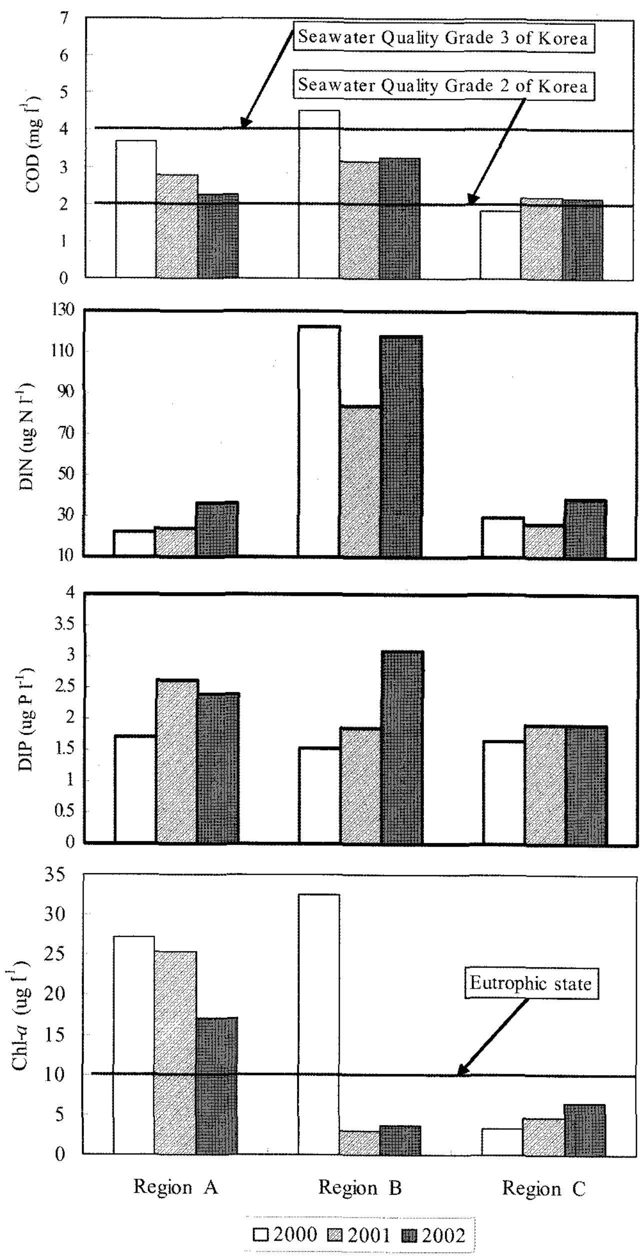

Fig. 2. Observed distribution of COD, DIN, DIP and Chl-a in the study area by NFRDI (National Fisheries Research & Development Institute).

characteristics of coastal waters are determined by freshwater discharges and pollutant loadings from terrestrial sources (Karageorgis *et al.* [2003]; Takeoka & Murao [1997]). On the other hand, in the semi-enclosed bay where shellfish are cultivated, land-based sources as well as benthic loads from fine-grained sediment are both responsible for the degradation of water quality.

To restore water quality or estimate TMDL, we need to calculate the required reduction in pollutant loads so as to engineer countermeasures against red tides and eutrophication (Lee *et al.* [2005]; Yanagi *et al.* [1997]). Studies of such water quality management practices have been conducted using numerical models including hydrodynamic and eutrophication models. These models simulate marine environmental factors by formulating the flow of ecosystem components in coastal waters (Cerco & Cole [1993]; Cerco [1995]; Drago *et al.* [2001]; Lee *et al.* [2005]; Lung [1988]; Mark & Bunch [1992]; Nakata & Taguchi [1982]; Taguchi & Nakata [1998]; Takeshi [1988]; Yanagi *et al.* [1997]). The present study advances previous research (Lee *et al.* [2005]). The model was applied to a broader area where different water types were present. In particular, the model was modified by the input of the maximum growth rate of phytoplankton (α_1), the maximum grazing rate of zooplankton (α_3), and the half-saturation constant for the uptake of PO_4^{3-}-P (K_{SP}) and DIN (K_{SN}), based on the spatial distribution of dominant species of phytoplankton and zooplankton, respectively.

Therefore, for effective water quality management in the study area, we predicted and evaluated summer water quality using a three-dimensional (3D) eco-hydrodynamic model. We then estimated the reduction in the amount of pollutant loads required to satisfy the water quality standards in each region, *i.e.*, below 10 μg l^{-1} Chl-*a* and 3 mg l^{-1} COD in Region A, below 10 μg l^{-1} Chl-*a* and 2 mg l^{-1} COD in Region B, and below 10 μg l^{-1} Chl-*a* and 1 mg l^{-1} COD in Region C.

2. MATERIALS AND METHODS

Marine physical and biogeochemical field observations were carried out in the summer seasons during the period 1996–1999 at stations A1 to C3 in the study area shown in Fig. 1. Observed water quality data and results were described by Lee [2000].

The coupled modeling of physical and biochemical processes, so-called 'eco-hydrodynamic modeling', serves as a powerful tool for assessing the water quality quantitatively in coastal regions (Taguchi & Nakata [1998]). The eco-hydrodynamic model consists of a multi-level model for water flow simulation and an ecological model for water quality simulation (Kremer & Nixon [1978]; Lee *et al.* [2005]; Nakata & Taguchi [1982]; Taguchi & Nakata [1998]). To suggest a plan for effective water quality management, tidal and residual currents were first simulated by the hydrodynamic model; after entering a residual current as a flow field into the ecological model, water quality compartments such as COD and phytoplankton biomass could be predicted.

2.1 Hydrodynamic model

In order to simulate the tidal and residual currents in the study areas, a well-developed hydrodynamic model (Nakata & Taguchi [1982]; Nakata *et al.* [1983]; Nakata *et al.* [1985]) was used. This model provides a 3D analysis of the physical processes in the inner bay and calculates the flow field for the ecological model. As described by Lee *et al.* [2005], the hydrodynamic model is made up of several equations: the momentum equation, which formulates the fluid dynamics in the inner bay and estuary; the continuity equation; the hydrostatic equation; the chloride mass balance equation; the heat flux equation and the equation of state, which formulates relationships with density, chloride and temperature in seawater. Finite difference methods were used to numerically evaluate the basic equations applied in this study. The flow velocity components were calculated at the sides of each grid cell, and the temperature, chlorinity, density and pressure were calculated at the cell centers (spatially staggered grid). Convective overturning was used, and the advection terms were computed using a combination of upstream and central difference schemes. The central difference scheme is mathematically more complex than the forward or backward difference schemes but produces more exact values. A set of suitable boundary conditions is required for the modeling. The non-slip condition was applied to the boundary layer that followed the coastline, and a free-slip condition was used along the width of the grid. The free-stream condition was applied to the velocity components along the open boundary. Other specific equations and boundary conditions, as well as the numerical scheme, are described in Nakata & Taguchi [1982].

2.2 Ecological model

The biochemical coupled model applied to our present work is essentially the same as one well described by Kremer & Nixon [1978] and Nakata & Taguchi [1982]. The model was developed to evaluate the physical–biological interactions in the estuarine lower trophic ecosystem in terms of nutrient and oxygen cycles, and extended to include the COD kinetics for purposes of water quality analysis. It is considered that the model is not a dynamic model, but a quasi-steady-state model that simulates equilibrium states at any given time in the water environment. The compartments of the ecological model are phytoplankton (P), zooplankton (Z), particulate organic carbon (POC) and dissolved organic carbon (DOC) for the organic forms; dissolved inorganic phosphorus (DIP) and dissolved inorganic nitrogen (DIN) for the inorganic forms; and dissolved oxygen (DO) and chemical oxygen demand (COD) for the water quality factors. The bottom environment associated with sediments, for instance benthic fluxes, is entered in terms of a variable as an environmental factor.

The variation in the concentrations of standing stock C at a given time in the ecological model is:

$\frac{\partial C}{\partial t}$ =advective transport + dispersive transport + biogeochemical variation

$$=-u\frac{\partial C}{\partial x}-v\frac{\partial C}{\partial y}-w\frac{\partial C}{\partial z}+\frac{\partial}{\partial x}\left(K_x\frac{\partial C}{\partial x}\right)+\frac{\partial}{\partial y}\left(K_y\frac{\partial C}{\partial y}\right)+\frac{\partial}{\partial z}\left(K_z\frac{\partial C}{\partial z}\right)+\frac{dC}{dt} \quad (1)$$

where C is the concentration of a compartment; t is time; u, v and w are mean velocity components; K_X, K_Y and K_Z are eddy diffusion coefficients; and dC/dt is the biogeochemical variation term. The standing stock of each compartment is predicted with temporal and spatial changes by entering velocity components calculated by hydrodynamic modeling into the ecological model. For example, the formulation of compartments is presented in Eqs. (2)–(9), respectively.

$$\frac{d}{dt}(P)=[1-\mu_3(P)]\cdot V_1(T)\cdot\mu_1(DIP,\ DIN)\cdot\mu_2(I)\cdot P - V_2(T)\cdot P - V_3(T)\cdot Z - V_4(T)\cdot P - W_P\frac{\partial}{\partial z}(P) \quad (2)$$

$$\frac{d}{dt}(Z)=V_3(T)\cdot Z-(1-m)\cdot V_3(T)\cdot Z-(m-n)\cdot V_3(T)\cdot Z-V_5(T)\cdot Z = [\nu\cdot V_3(T) - V_5(T)]\cdot Z - W_Z(t)\frac{\partial}{\partial z}(Z) \quad (3)$$

$$\frac{d}{dt}(POC) = -W_{POC}\frac{\partial}{\partial z}(POC)-V_6(T)\cdot(POC)+V_4(T)\cdot P +(1-m)\cdot V_3(T)\cdot Z+V_5(T)\cdot Z+Q_{POC} \quad (4)$$

$$\frac{d}{dt}(DOC)=\mu_3(P)\cdot V_1(T)\cdot\mu_1(DIP,\ DIN)\cdot\mu_2(I)\cdot P +\frac{1}{1+k}(k\cdot V_6(T)\cdot(POC))-V_7(T)\cdot(DOC)+Q_{DOC} \quad (5)$$

$$\frac{d}{dt}(DIN) = -[N:C_P]\cdot V_1(T)\cdot\mu_1(DIP,\ DIN)\cdot\mu_2(I)\cdot P + [N:C_{POM}]\frac{1}{1+k}V_6(T)\cdot(POC)+ [N:C_P]\cdot V_2(T)\cdot P + [N:C_Z](\mu-\nu)\cdot V_3(T)\cdot Z + [N:C_{DOM}]\cdot V_7(T)\cdot(DOC)+Q_N \quad (6)$$

$$\frac{d}{dt}(DIP) = -[P:C_P]\cdot V_1(T)\cdot\mu_1(DIP,\ DIN)\cdot\mu_2(I)\cdot P + [P:C_{POM}]V_6(T)\cdot(POC) +[P:C_P]\cdot V_2(T)\cdot P + [P:C_Z]\cdot(\mu-\nu)\cdot V_3(T)\cdot Z +[P:C_{DOM}]\cdot V_7(T)\cdot(DOC)+Q_P \quad (7)$$

$$\frac{d}{dt}(COD)=[COD:C_P](\frac{dP}{dt})+[COD:C_Z](\frac{dZ}{dt})+[COD:C_{POM}](\frac{dPOC}{dt}) +[COD:C_{DOM}](\frac{dPOC}{dt}) \quad (8)$$

$$\frac{d}{dt}(DO)=+[TOD:C_P]]\cdot V_1(T)\cdot\mu_1(DIP,\ DIN)\cdot\mu_2(I)\cdot P +K_a(DO_S-DO)-[TOD:C_P]]\cdot V_2(T)\cdot P -[TOD:C_Z]\cdot(\mu-\nu)\cdot V_3(T)\cdot Z-[TOD:C_{POM}]\cdot V_6(T)\cdot(POC) -[TOD:C_{DOM}]\cdot V_7(T)\cdot(DOC)-[TOD:C_B]\cdot V_8(T)\cdot D_B \quad (9)$$

where $V_1(T)$ is the maximum growth rate of phytoplankton ($\alpha_1 \exp(\beta_1\cdot T)$); μ_1(DIP, DIN), nutrient limitation of phytoplankton $\left[\min\left(\frac{N}{K_{SN}+N'}, \frac{P}{K_{SP}+P}\right)\right]$; $\mu_2(I, P)$, light availability ($\frac{I_0(t)}{I_{opt}}\exp^{-kz}\cdot\exp[1-\frac{I_0(t)}{I_{opt}}\exp^{-kz}$, $I_0(t)=I_{max}\cdot\sin^3(\frac{\pi}{DL}\cdot t)]$; $\mu_3(P)$, extracellular release of phytoplankton ($0.135\ \exp[-0.00201\cdot(\text{Chl-}a:C_P)\cdot P]$); $V_2(T)$, respiration rate of phytoplankton ($\alpha_2 \exp(\beta_2\cdot T)$); $V_3(T)$, maximum grazing rate of zooplankton ($\alpha_3 \exp(\beta_3\cdot T)\{1-\exp[\lambda(P^*-P)]\}$); $V_4(T)$, death rate of phytoplankton ($\alpha_4 \exp(\beta_4\cdot T)$); $V_5(T)$, natural death rate of zooplankton ($\alpha_5 \exp(\beta_5\cdot T)$); $W_P\frac{\partial}{\partial z}(P)$, settling flux of phytoplankton; $W_Z(t)\frac{\partial}{\partial z}(Z)$, diurnal vertical movement of zooplankton; $V_6(T)$, mineralization rate of POC ($\alpha_6 \exp(\beta_6\cdot T)\frac{DO}{K^1_{DO}+DC}$; $V_7(T)$, mineralization rate of DOC($\alpha_7 \exp(\beta_7\cdot T)\frac{DO}{K^2_{DO}+DC}$; $V_8(T)$, oxygen consumption rate of sediment ($\alpha_8 \exp(\beta_8\cdot T)$); T, water temperature; t, time; z, depth; Q_{POC}, Q_{DOC}, Q_N and Q_P are POC, DOC, DIN and DIP input loads from the sources, respectively. The definitions and input values of parameters used are listed in Table 1.

3. MODELING INPUT DATA

The spatially staggered grid (Arakawa C) system was adopted to model the study area. The X- and Y-axes were divided into 154 and 63 grids, respectively, and the Z direction was divided into three levels in consideration of the thermocline (Level 1, 0–5 m; Level 2, 5–15 m; Level 3, below 15 m). The horizontal grid scale was 500 m, and the open boundary was established as the line BD-1 and BD-2, as shown in Fig. 1.

3.1 Hydrodynamic model

Input data for the hydrodynamic model are summarized in Table 2. M_2, the prevailing harmonic component, was used, and the values for bottom friction coefficient, horizontal diffusion coefficient and vertical diffusion coefficient were based on typical values cited in the model documentation (Lee *et al.* [2005]; Nakata & Taguchi [1982]; Nakata *et al.* [1983]; Nakata *et al.* [1985]). Also, the f-plane approximation was used by which the Coriolis coefficient is constant with latitude.

3.2. Ecological model

Initial and boundary values for the ecological model are summarized in Table 3. The same values of horizontal and vertical diffusion coefficients were used that were applied in the hydrodynamic model. As shown in Fig. 1, 45 land-based pollution sources, such as rivers, ditches, sewage and wastewater entering the sea, were identified, and analyzed pollutant loads for each compartment are shown in Table 4. Non-point sources were not considered. As benthic fluxes from sediment, NH_4^+-N and PO_4^{3-}-P were inputted in the ranges 14.87–36.37 mg m^{-2} day^{-1} and 7.04–9.90 mg m^{-2} day^{-1}, respectively, with special

Table 1. Definition and input values of biological parameters used in the ecological model

Symbol	Definition	Unit	Input values	Typical values	Remarks
α_1	Maximum growth rate of phytoplankton at 0°C	day^{-1}	0.300-1.400	0.060-5.650	Jorgensen [1979]
β_1	Temperature coefficient	$^{o}C^{-1}$	0.0633		
α_2	Respiration rate of phytoplankton at 0°C	day^{-1}	0.010	0.030-0.051	Di Toro et al. [1971]
β_2	Temperature coefficient	$^{o}C^{-1}$	0.052		
α_3	Maximum grazing rate of zooplankton at 0°C	day^{-1}	0.05-0.18	0.18	Baca and Arnett [1976]
β_3	Temperature coefficient	$^{o}C^{-1}$	0.058		
α_4	Death rate of phytoplankton at 0°C	day^{-1}	0.015	0.096-0.330	Baca and Arnett [1976]
β_4	Temperature coefficient	$^{o}C^{-1}$	0.0693		
α_5	Natural death rate of zooplankton at 0°C	day^{-1}	0.050	0.003-0.096	Scavia and Eadie [1976]
β_5	Temperature coefficient	$^{o}C^{-1}$	0.0693		
α_6	Mineralization rate of POC at 0°C	day^{-1}	0.085	0.001-0.237	Ishikawa and Nishimura [1983]
β_6	Temperature coefficient	$^{o}C^{-1}$	0.041		
α_7	Mineralization rate of DOC at 0°C	day^{-1}	0.002	0.013-0.043	Ogura [1975]
β_7	Temperature coefficient	$^{o}C^{-1}$	0.0693		
α_8	Oxygen consumption rate of sediment at 0°C	day^{-1}	1.000		
β_8	Temperature coefficient	$^{o}C^{-1}$	0.0693		
K_{SP}	Half saturation constant for uptake of PO43- at 0°C	$\mu g\ P\ l^{-1}$	0.024-0.150	0.008-0.530	O'Connor et al. [1975]
K_{SN}	Half saturation constant for uptake of PO43- at 0°C	$\mu g\ N\ l^{-1}$	0.400-1.100	0.300-1.462	Di Toro et al. [1971]
I_{opt}	Optimum intensity of radiation for photosynthesis	$ly\ day^{-1}$	200.0-250.0		
I_{max}	Maximum intensity of sunlight at sea surface	$Cal\ cm^{-2}\ day^{-1}$	551.6-632.1		Observed
D	Length of day	day	0.500		
k_0	Dissipation coefficient of light independent of Chl-*a*	m^{-1}	0.570		
k_1	Constant of dissipation coefficient depending on Chl-*a*	$m^{-1}(mgChl\text{-}a\ m^{-3})^{-1}$	0.0179		
λ	Ivlev index of zooplankton grazing	$(mg\ C\ m^{-3})^{-1}$	0.007		
P^*	Function of grazing	$mg\ C\ m^{-3}$	70.0	40.0-190.0	
μ	Digestion efficiency of zooplankton	%	70.0	39.0-98.0	Di Toro et al. [1971]
ν	Total growth efficiency of zooplankton	%	30.0	4.0-50.0	
K	Percentage of the quantity decomposed from POC to DOC	%	29.0	21.0-35.0	Ishikawa and Nishimura [1983]
K^1_{DO}	Half concentration of DO for mineralization of POC	$mg\ l^{-1}$	1.000	0.0035-1.000	
K^2_{DO}	Half concentration of DO for mineralization of POC	$mg\ l^{-1}$	1.000	0.0035-1.000	
W_P	Settling velocity of phytoplankton	$m\ day^{-1}$	0.350	0.173-1.350	Jorgensen [1979]
W_{POC}	Settling velocity of detritus (POC)	$m\ day^{-1}$	1.1	0.0-2.0	Jorgensen [1979]

distributions observed in each region. Definitions of major parameters and input values based on typical values cited in references are summarized in Table 1 (Bowie *et al.* [1985]; Lee [2000]). Using the input conditions, calibration was achieved when we obtained reasonable agreement between model results and observed data. Quasi-steady state was obtained 100 days after the beginning of the calculation.

4. RESULTS AND DISCUSSION

To verify the result of currents calculated by the hydrodynamic model, we compared simulated to observed tidal current ellipses at stations EC1, EC4 and EC5 shown in Fig. 1 (Fig. 3). Because the patterns in flow velocity and direction were similar, it was estimated that the hydrodynamic model simulated the flow field of the study area quite well. Residual currents can have a great influence on the long-term distribution of material in coastal areas and are dominated by tidally-induced residual currents, wind-driven currents and density-driven currents. The surface distribution of residual currents that played an important role in coastal zones is shown in Fig. 4. Water flow was stagnant, with a velocity of 2 cm s^{-1} in the inner bay,

Table 1. (continued)

Symbol	Definition	Unit	Input values	Typical values	Remarks
W_Z^1	Maximun upward velocity at night for diurnal perpendicular motion of zooplankton	m day^{-1}	18.1		
W_Z^2	Maximun downward velocity in the daytime for diurnal perpendicular motion of zooplankton	m day^{-1}	18.1		
K_a	Reaeration coefficient at sea surface	day^{-1}	0.250		
DO_S	Saturation concentration of DO	mg l^{-1}	7.0		Observed
D_B	Quantity of deposit in sediment	mg C m^{-2}	222.5	variable	
[P:C_P]	Ratio of P/C for phytoplankton	weight ratio	3.500E-4	variable	
[N:C_P]	Ratio of N/C for phytoplankton	weight ratio	1.171E-3	variable	
[TOD:C_P]	Ratio of TOD/C for phytoplankton	weight ratio	3.470E-3	variable	
[COD:C_P]	Ratio of COD/C for phytoplankton	weight ratio	1.535E-3	variable	
[Chl-*a*:C_P]	Ratio of Chl-*a*/C for phytoplankton	weight ratio	0.032	variable	
[P:C_Z]	Ratio of P/C for zooplankton	weight ratio	7.040E-4	variable	
[N:C_Z]	Ratio of N/C for zooplankton	weight ratio	1.320E-2	variable	
[TOD:C_Z]	Ratio of TOD/C for zooplankton	weight ratio	3.510E-3	variable	
[COD:C_Z]	Ratio of COD/C for zooplankton	weight ratio	1.553E-3	variable	
[P:C_{POC}]	Ratio of P/C for POC	weight ratio	5.048E-4	variable	
[N:C_{POC}]	Ratio of N/C for POC	weight ratio	9.921E-3	variable	
[TOD:C_{POC}]	Ratio of TOD/C for POC	weight ratio	3.300E-3	variable	
[COD:C_{POC}]	Ratio of COD/C for POC	weight ratio	1.460E-5	variable	
[P:C_{DOC}]	Ratio of P/C for DOC	weight ratio	2.581E-4	variable	
[N:C_{DOC}]	Ratio of N/C for DOC	weight ratio	7.143E-3	variable	
[TOD:C_{DOC}]	Ratio of TOD/C for DOC	weight ratio	3.120E-3	variable	
[COD:C_{DOC}]	Ratio of COD/C for DOC	weight ratio	1.381E-5	variable	
[TOD:C_B]	Ratio of TOD/C in deposit of sediment	weight ratio	2.667	variable	

Table 2. Input data for the hydrodynamic model

Parameters	Input values
Mesh size	$\Delta X = \Delta Y = 500$ m
Water depth	Chart datum + Mean sea level
Time interval	10 sec
Level thickness	Level 1: 0-5 m
	Level 2: 5-15 m
	Level 3: below 15 m
Tidal amplitude and phase at open boundary (M_2)	BD-1: 65.20 cm, 242.60° BD-2: 28.48 cm-49.90 cm, 228.20°-243.90°
Water temp. and chlorinity at open boundary	Level 1: 22.10°C, 17.10 ‰
	Level 2: 21.20°C, 16.66 ‰
	Level 3: 21.20°C, 17.27 ‰
Coriolis coefficient	$f = 2\omega\sin\varphi$
Surface friction coefficient	0.0013
Internal friction coefficient	0.0013
Bottom friction coefficient	0.0025
Horizontal viscosity coefficient	1.0E6 (cm^2 s^{-1})
Horizontal diffusion coefficient	1.0E6 (cm^2 s^{-1})
Calculation time	10 tidal cycles

and offshore water flowed in at a maximum rate of 5 cm s^{-1} through boundary D. Counter-clockwise gyres existed in the central part of Region A. The patterns in Region B, however, differed considerably from those in the other regions. Effluent was spread strongly, with a maximum velocity of 7 cm s^{-1}, to the south end of the Gadeokdo through summer daily discharge (about 55,000,000 tons day^{-1}) from the Nakdong River, and some flowed into Region A at about 5 cm s^{-1} through the strait of Gadeok. The influence of freshwater discharge from the Nakdong River greatly impacted Region B. It is suggested that the residence time of materials inside Region B may be very short because of strong advection and diffusion. Inside Region C, the water was stagnant, but the flow velocity increased towards offshore areas. Water flow in a northeasterly direction with a velocity >5 cm s^{-1} was simulated offshore of the study area.

The stability of the solutions and calibration were assessed after we entered residual currents into the flow field of the ecological model. To verify summer water quality patterns with the ecological model, we compared the predicted values of Chl-*a*, COD, DIN and DIP with the observed values at stations in each region. The results are shown in Fig. 5. The values of relative error (RE) of Chl-*a* ranged from 1.4% to 46.4%, with mean values of 14.0% in Region A, 26.7% in Region B, and 19.4% in Region C, indicating that summer distribution

Table 3. Input data for the ecological model

Parameters								
Time interval					450 sec			
Pollutant loads					Refer to Table 4			
Initial values for compartments								
Level	DO (mg l^{-1})	COD	DIP (μg P l^{-1})	DIN (μg N l^{-1})	POC	DOC (mg C m^{-3})	PHYTO	ZOO
1	5.77-12.09	0.58-8.18	0.07-3.27	0.23-176.39	132.35-2,000.00	1,170.00-3,255.00	27.90-1,081.60	50.00
2	4.39-9.63	1.28-5.76	0.13-2.92	0.09-61.82	125.20-500.00	780.00-2,719.00	28.40-596.70	50.00
3	1.62-8.83	1.08-5.64	0.15-2.06	4.37-40.29	74.05-500.00	800.00-2,558.00	6.00-393.60	100.00
Boundary values for compartments								
Level	DO (mg l^{-1})	COD	DIP (μg P l^{-1})	DIN (μg N l^{-1})	POC	DOC (mg C m^{-3})	PHYTO	ZOO
BD-2 1	9.29-10.66	1.75	0.07-0.26	0.23-2.09	132.35	2,570.00	27.90-276.20	50.00
BD-2 2	8.21-9.03	1.50	0.16-0.58	0.09-8.61	125.20	2,575.00	28.40-75.60	50.00
BD-2 3	7.70-8.83	1.42	0.32-0.55	4.37-14.27	74.05	1,370.00	6.00-12.00	100.00
BD-1 1	8.95	1.92	0.39	9.53	2,460.00	2,540.00	127.80	50.00
BD-1 2	4.52	2.07	0.83	5.65	2,010.00	2,595.00	95.30	50.00
BD-1 3	1.36	1.91	1.16	7.40	1,560.00	2,650.00	62.30	100.00
Horizontal viscosity coefficient and diffusion coefficient					Level 1: 1.0E6 (cm^2 s^{-1}) Level 2: 1.0E5 (cm^2 s^{-1}) Level 3: 1.0E4 (cm^2 s^{-1})			
Vertical diffusion coefficient					Level 1-3: 0.1 (cm^2 s^{-1})			
Water Temperature and Salinity					Level 1: 22.47-25.46, 3.38-34.02 psu Level 2: 17.22-22.47, 28.42-34.11 psu Level 3: 13.60-19.91, 29.97-34.45 psu			
Calculation time					200 tidal cycles			

patterns and absolute values of phytoplankton in the study area were quite well reproduced by the ecological model. Relatively high RE values in Region B were due to the limited ability to predict water quality due to sudden freshwater discharges when the estuarine barrage was opened. Mean RE values of COD were 28.7%, 24.9% and 16.3% in Regions A, B and C, respectively. Mean RE values of DIN and DIP at some stations in each region were 45% and 51%, respectively, which are considerably higher than the values of Chl-*a* and COD. The overall distribution patterns, however, were similar to the observed patterns, with the exception of DIP in Region A. This high RE was a result of focusing on organic matter, such as Chl-*a* and COD, in the calibration of the model. Also, *r*-values indicate interrelationships between the observed and simulated values; these were 0.9451, 0.6841, 0.9536 and 0.5705 for Chl-*a*, COD, DIN and DIP, respectively. Taken together, even though there were some gaps between each of the stations, it is suggested that the distribution patterns and absolute values of Chl-*a* and COD in the study area were quite well reproduced by the ecological model. When verifying the model for studying water quality management in a bay, it is reasonable to consider the entire water quality pattern and mean values rather than the results of particular stations. It is noteworthy that validation of all compartments is very difficult in ecological modeling. In this study, we focused on Chl-*a*, a eutrophication index, and COD as seawater quality criteria in Korea. To improve the ecological model, modifications to the limits of the model and the study approach are necessary, *i.e.* accuracy of input data and parameters and modification of the model itself must be achieved. Because of the agreement between absolute values and distribution patterns such as Chl-*a* and COD, the results of the ecological model were acceptable.

The results of a sensitivity analysis of the ecological model are presented in Table 5. We calculated the concentration values of the Chl. *a* and DIN when the initial values of the major parameters were increased or decreased by 50%. We also changed the set concentration value of the parameter that had the largest effect by 100% and calculated the effect on the other coefficients in terms of a saturation percentage. The parameter that had the largest effect on the Chl. *a* and DIN was maximum growth rate of phytoplankton (α_1). Also, death rate, respiration rate, and settling velocity of phytoplankton

Table 4. Terrestrial pollutant loads from point sources flowing into the model region

Name of point sources		Flowrate (ton day^{-1})	COD (ton day^{-1})	DO (ton day^{-1})	DIP (kg day^{-1})	DIN (kg day^{-1})	POC (kg day^{-1})	DOC (kg day^{-1})
Region A	R 1	77,947.0	1.53	0.64	33.40	462.28	720.0	1,400.0
	R 2	33,917.0	0.39	0.30	9.73	170.19	720.0	1,400.0
	R 3	426,222.0	3.44	3.96	30.77	3,678.91	720.0	1,400.0
	R 4	15,448.0	0.45	0.10	3.51	60.88	720.0	1,400.0
	R 5	27,864.0	0.69	0.17	36.74	313.42	720.0	1,400.0
	R 6	59,088.0	0.74	0.60	10.67	577.20	720.0	1,400.0
	R 7	10,071.0	0.22	0.09	1.55	71.94	720.0	1,400.0
	R 8	7,366.5	0.36	0.06	8.96	111.42	720.0	1,400.0
	R 9	44,578.5	1.65	0.21	408.91	761.33	720.0	1,400.0
	R 10	54,658.5	0.83	0.50	35.49	604.71	720.0	1,400.0
	R 11	55,987.0	1.59	0.44	63.61	739.37	2,500.0	500.0
	R 12	15,915.5	0.61	0.10	10.86	127.88	2,420.0	502.0
	R 13-21	520,640.0	121.40	28.43	4,882.03	30,588.07	21,780.0	4,518.0
	R 22	18,096.5	0.04	0.17	2.70	291.65	2,420.0	502.0
	R 23	14,645.0	0.01	0.16	1.20	1674.34	2,420.0	502.0
	R 24	8,825.5	0.002	0.09	1.15	435.69	1,000.0	2,000.0
	R 25	46,801.5	0.08	0.45	8.29	433.21	1,000.0	2,000.0
	R 26-27	160,450.0	0.90	3.50	39.17	237.70	2,000.0	4,000.0
	R 28	341,092.5	0.65	3.55	27.87	3,675.19	1,000.0	2,000.0
	R 29	12,169.0	0.04	0.14	2.36	116.59	1,000.0	2,000.0
	R 30	15,416.0	0.07	0.18	3.41	104.08	1,000.0	2,000.0
	R 31	20,714.5	0.06	0.18	6.04	378.33	1,000.0	2,000.0
	R 32	139,395.5	0.55	1.48	23.24	2,013.94	1,000.0	2,000.0
	R 33	115,002.0	0.82	0.96	28.13	1,649.50	1,000.0	2,000.0
	R 34	154,945.0	0.65	1.56	17.96	2,213.28	1,000.0	2,000.0
	R 36	7,032.5	0.08	0.06	3.07	155.89	1,000.0	2,000.0
	R 37	6,830.0	0.02	0.09	1.10	56.83	1,000.0	2,000.0
	R 38	9,419.0	0.05	0.10	0.87	50.64	1,000.0	2,000.0
	R 39	41,472.0	0.27	0.42	3.07	319.96	600.0	1,000.0
	R 40	25,920.0	0.07	0.31	2.81	293.57	600.0	1,000.0
	R 41	29,292.0	0.15	0.33	2.38	306.86	600.0	1,000.0
	R 42	45,097.5	0.18	0.46	1.35	262.34	600.0	1,000.0
	R 43	153,405.0	0.45	1.57	10.64	2,468.67	600.0	1,000.0
	R 44	20,768.5	0.12	0.22	2.32	321.01	600.0	1,000.0
	R 45	11,761.0	0.06	0.12	0.63	136.31	600.0	1,000.0
	R 46	20,723.0	0.08	0.21	1.25	202.50	567.0	1,000.0
	R 47	18,788.0	0.12	0.18	7.35	159.14	567.0	1,000.0
	R 48	126,384.5	0.68	1.22	19.87	1,001.69	567.0	1,000.0
	R 49-50	289,088.5	3.25	5.61	58.36	3,829.93	1,134.0	2,000.0
Region B	Nakdong R.	55,344,014.8	343.13	418.95	4,704.24	189,110.50	201,452.2	316,014.3
	Jangrim W.W.T.P.	302,492.9	7.41	2.26	320.00	16,020.00	1,132.3	3,396.9
Region C	Bosou R.	62,201.0	2.38	0.16	88.33	661.20	124.4	248.8
	Dong R.	329,184.0	12.57	0.86	467.44	3,499.23	658.4	1,316.7
	Souyong R.	501,984.0	4.56	2.22	555.90	10,062.80	1,111.9	3,335.7
	Nampu W.W.T.P.	566,152.0	6.96	2.26	611.40	7,897.80	1,132.3	3,396.9

were largely contributed to Chl. *a*. However, for the DIN, mineralization rates of POC and DOC had large effect. Thus, we concluded that coefficients related to phytoplankton in the Chl. *a* and DIN were important.

The simulated distribution of Chl-*a*, COD, DIN and DIP based on the ecological model are shown in Fig. 6. The con-

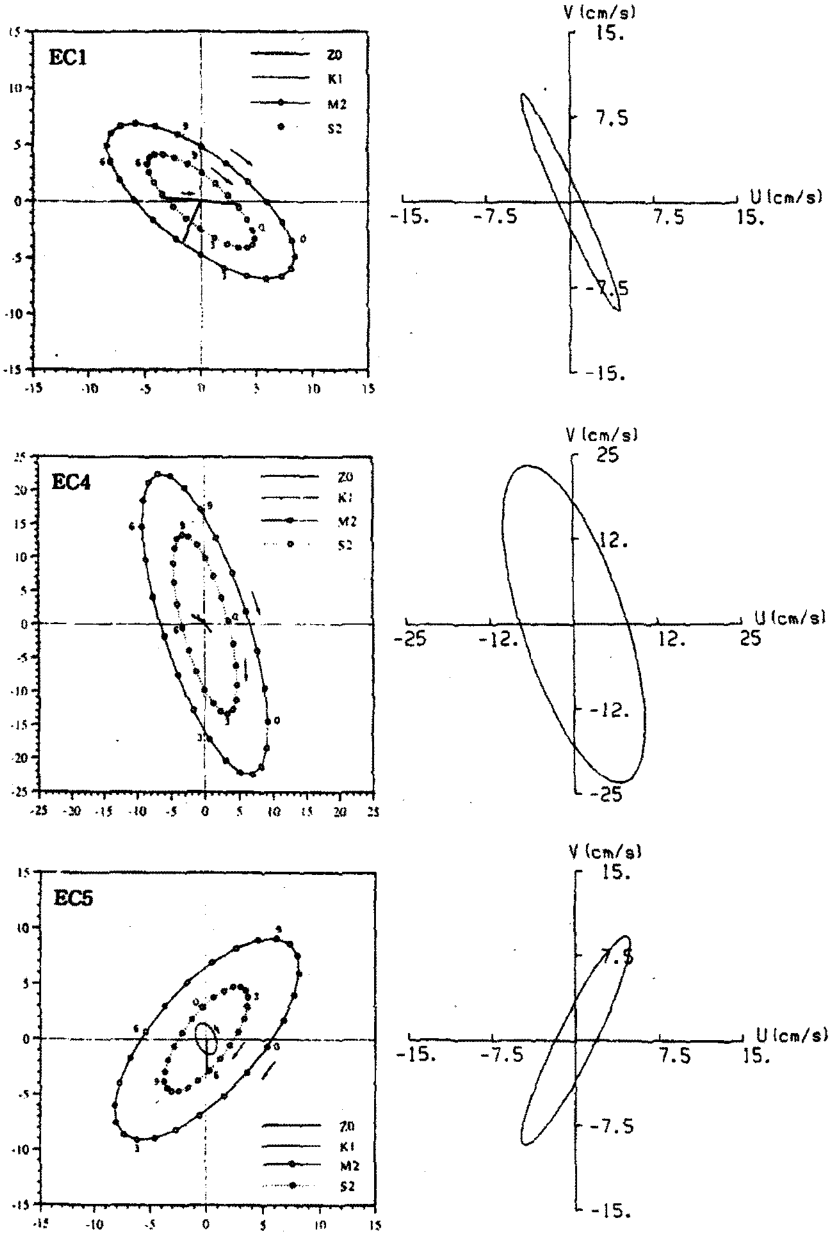

Fig. 3. Comparison of the tidal current ellipses between observed (left) and computed (right) results.

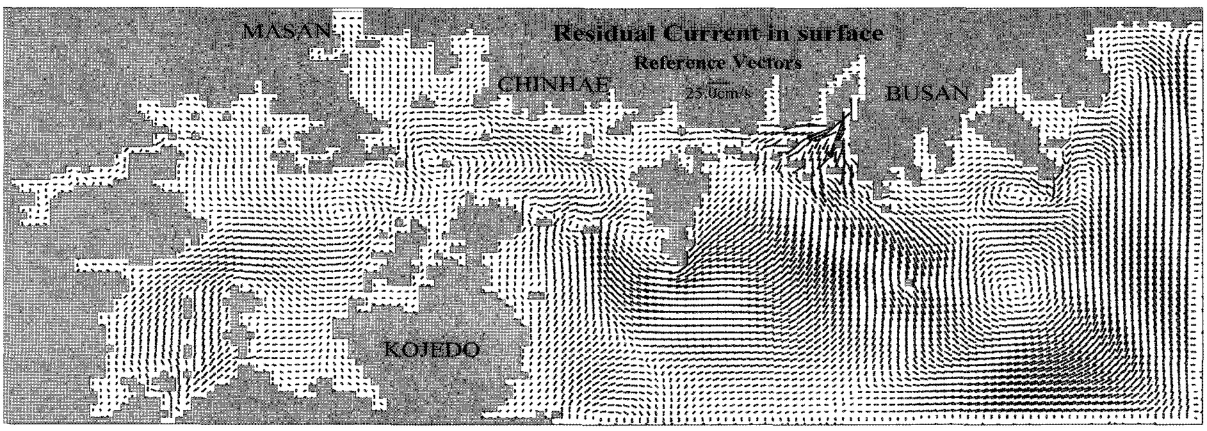

Fig. 4. Computed residual currents at surface level in the study area.

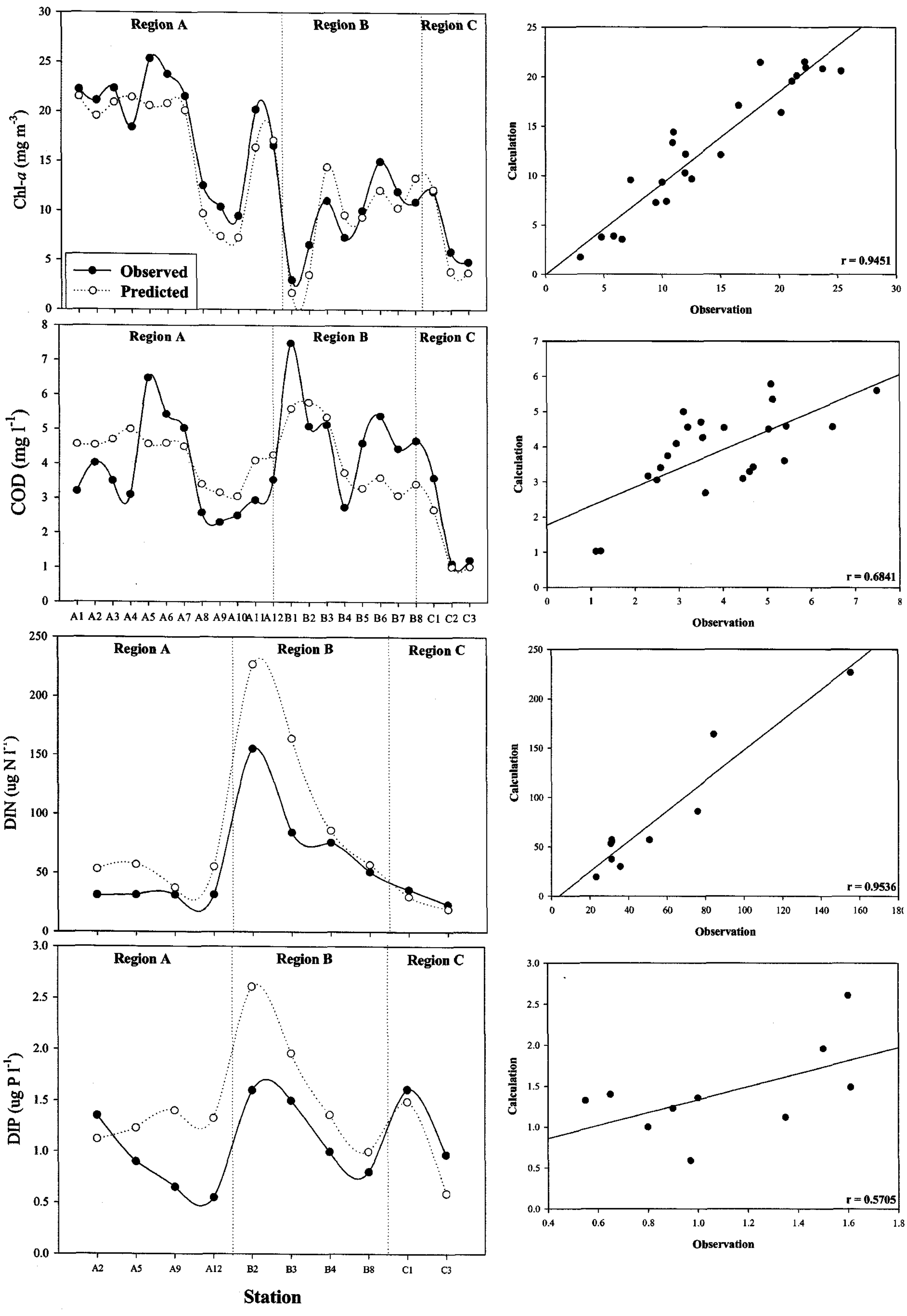

Fig. 5. Comparison of simulated results with observed Chl-*a*, COD, DIN and DIP values at surface level in the study area.

Table 5. Sensitivity analysis for the reaction coefficient in the ecological model: We changed the set concentration value of the parameter that had the largest effect by 100% and calculated the effect on the other coefficients in terms of a saturation percentage

Major Coefficients	Percentage contribution to simulated Chl. *a* concentrations (%)	Percentage contribution to simulated DIN concentrations (%)
Maximum growth rate of phytoplankton at 0°C	100.0	100.0
Respiration rate of phytoplankton at 0°C	11.2	15.3
Maximum grazing rate of zooplankton at 0°C	3.7	0.6
Death rate of phytoplankton at 0°C	20.5	5.7
Mineralization rate of POC at 0°C	0.1	73.3
Mineralization rate of DOC at 0°C	0.1	38.8
Half saturation constant for uptake of PO_4^{3-} at 0°C	0.9	1.3
Half saturation constant for uptake of DIN at 0°C	0.1	0.7
Settling velocity of phytoplankton	10.4	17.2
Ratio of N/C for phytoplankton	0.0	19.9

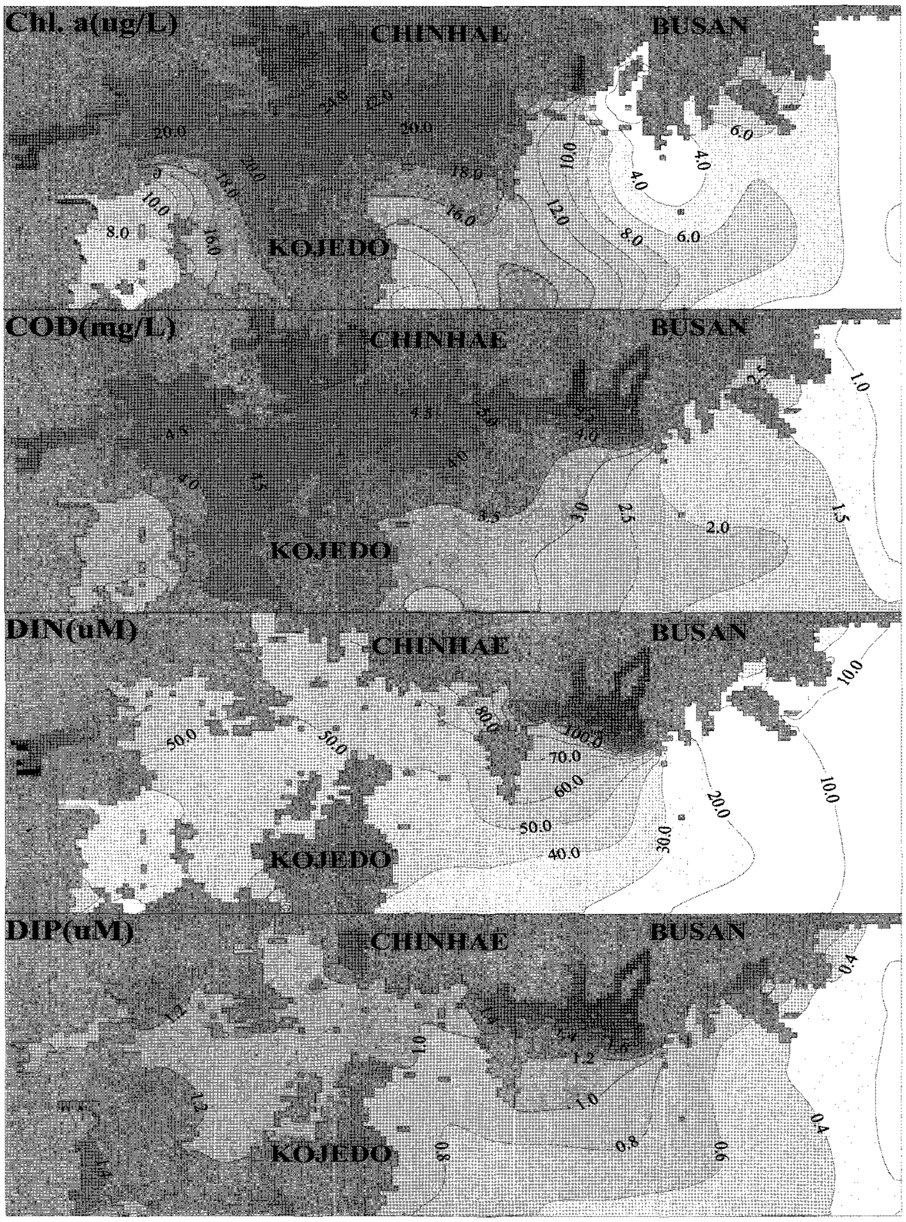

Fig. 6. Simulation results of surface Chl-*a*, COD, DIN and DIP values in the study area in summer.

centrations of Chl-*a* were above 10 μg l^{-1} at all sites in Region A and increased above 20 μg l^{-1} in the inner bay where pollutant loads were very large and water flow was stagnant. On the other hand, Chl-*a* was <4 μg l^{-1} in Region B because of a sudden freshwater discharge from the estuarine barrage, and it increased in offshore areas. Region C showed a homogeneous Chl-*a* distribution around 8 μg l^{-1}. In Region A, COD was >4 mg l^{-1}, which exceeded water quality Grade III, due to a phytoplankton bloom, indicating that the organic content of the water column in Region A was very high. Also, COD in the inner area of Region B exceeded 5 mg l^{-1} due to polluted freshwater input, even though Chl-*a* was low. Sustainable management of pollution of the Nakdong River is necessary to restore water quality standards. COD in Region C was low compared to values in the other regions. Nonetheless, water quality management for recovery of Grade I is necessary. The distribution of DIN was <50 μg N l^{-1} in Region A and <10 μg N l^{-1} in Region C, while steep concentration clines existed in Region B in the range of 50–200 μg N l^{-1}. DIP showed patterns similar to those of DIN. From the numerical experiment and observations, input of inorganic and organic substances to Region B was considered very high. Summer mean values of Chl-*a* in Regions A, B and C were 17, 8 and 6 μg l^{-1}, and COD values were 4.1, 4.2 and 1.5 mg l^{-1}, respectively. That is, under current environmental conditions, in particular, pollutant loadings to the study area were high, COD exceeded seawater quality criteria, and the water was either already eutrophic or in the process of becoming eutrophic. Therefore, it is necessary to estimate the decrease in pollutant loads required to restore and manage water quality in each region of the study area using a numerical model. Suitable target limits for water quality recovery or reductions in pollutant loads are <10 μg l^{-1} Chl-*a* and 3 mg l^{-1} COD in Region A, <10 μg l^{-1} Chl-*a* and 2 mg l^{-1} COD in B, and <10 μg l^{-1} Chl-*a* and 1 mg l^{-1} COD in C.

As shown in Fig. 7, when we reduced the COD, inorganic nitrogen and phosphorus loads from land only by 90%, the water quality criteria of Region A were not satisfied due to high background concentrations in the bay itself, as well as input loads. If, however, nutrient loads (input values of NH_4^+-N and PO_4^{3-}-P were about 36.37 mg m^{-2} day^{-1} and 9.90 mg m^{-2} day^{-1}, respectively) from polluted sediment were reduced by 70%, and terrestrial loads were simultaneously reduced by 70%, COD and Chl-*a* were restored. That is, sediment controls are significant for water quality management of this area where red tide outbreaks are frequent and intensive aquaculture is

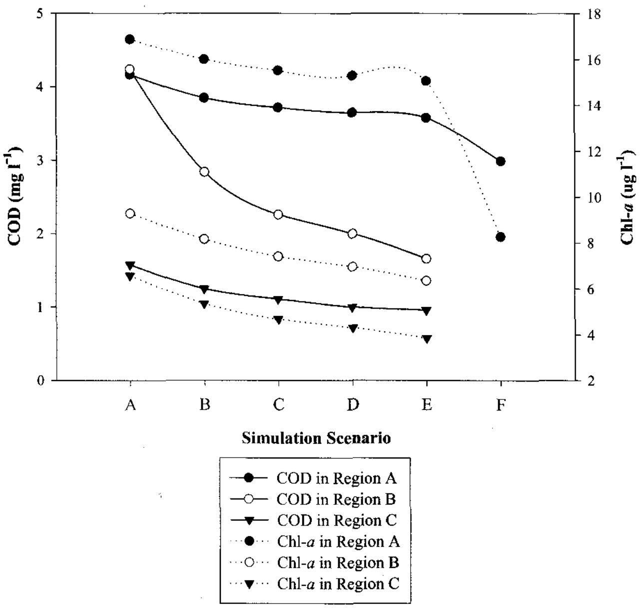

Fig. 7. Estimation of pollutant-load reduction on Chl-a and COD restoration in the study area; A: present situation; B: (COD+DIN+DIP) 50% reduction in land-based pollution sources; C: (COD+DIN+DIP) 70% reduction in land-based pollution sources; D: (COD+DIN+DIP) 80% reduction in land-based pollution sources; E: (COD+DIN+DIP) 90% reduction in land-based pollution sources; F: (COD + DIN+DIP) 70% reduction in land-based pollution sources and [NH_4^++PO_4^{3-}] 70% reduction in nutrient loads from polluted sediments.

conducted. Continuous development and study of restoration techniques, such as aeration, dredging, plowing, etc., to improve the polluted sediment are necessary. When we reduced the input COD and nutrient loads from the Nakdong River by 80%, Chl-*a* and COD in Region B fell below 10 μg l^{-1} and 2 mg l^{-1}, respectively. Therefore, prevention of eutrophication of the Nakdong River is very important to water quality management. The water quality criteria of Region C were satisfied when we reduced the COD and nutrient loads from land only by 70%.

Based on these results, terrestrial total allowable loadings of COD and inorganic nutrients in each region were determined by multiplying these reduction rates by current pollutant loads (Table 6). Those of COD, DIN and DIP in Region A were estimated at 43,005, 18,317 and 1,744 kg day^{-1}, respectively; 70,108, 41,026 and 1,005 kg day^{-1} in Region B; and 7,941, 6,636 and 517 kg day^{-1} in Region C. Also, total allowable NH_4^+-N and PO_4^{3-}-P loads from sediment in Region A were estimated at about 10.01 and 2.97 mg m^{-2} day^{-1}, respectively.

Estimated very high reduction rates, although difficult to achieve at the present time in relation to current environmental conditions, suggest that water pollution is very severe in this

Table 6. Estimation of terrestrial total allowable pollutant loads of COD and inorganic nutrient in the study area (in addition, total allowable NH_4^+-N and PO_4^{3-}-P loads from sediment in Region A were estimated at about 10.01 and 2.97 mg m^{-2} day^{-1}, respectively)

Region	Current pollutant loads (kg day^{-1})			Total allowable pollutant loads (kg day^{-1})		
	COD	DIN	DIP	COD	DIN	DIP
A	143,350.00	61,056.44	5,812.82	43,005.00	18,316.93	1,743.85
B	350,540.00	205,130.50	5,024.24	70,108.00	41,026.10	1,004.85
C	26,470.00	22,121.03	1,723.07	7,941.00	6,636.31	516.92

study area, and pollutant loads must be reduced within total allowable loads by continuous and long-term management. This abatement of quantitative pollutant loads based on numerical modeling is useful for water quality management practices. To achieve TMDL, sustainable countermeasures are necessary, including the expansion of sewage and wastewater facilities, effective removal of nutrients by advanced treatment, polluted sediment control measures and limited land use. And, the policy that not pollutant concentration control but total pollutant load control from sources should be executed in coastal areas for water pollution countermeasures and environmental management as quickly as possible.

5. CONCLUSIONS

Under the current environmental conditions, in particular, pollutant loadings to the study area were very high, and water quality was in a eutrophic condition. A three-dimensional eco-hydrodynamic model is used to predict water quality in summer and to estimate the reduction rate in pollutant loads that would be required to restore water quality. The model reproduced reasonably the flow field and water quality of the study area.

When the nutrient loads from polluted sediment and land were each reduced by 70% simultaneously, COD and Chl-*a* of Region A were restored. When we reduced the input COD and nutrient loads from the Nakdong River by 80%, Chl-*a* and COD of Region B decreased below 10 μg l^{-1} and 2 mg l^{-1}, respectively. The water quality criteria of Region C were satisfied when we reduced the terrestrial COD and nutrient loads by 70%. Total allowable loadings of COD and inorganic nutrients in each region were determined by multiplying the reduction rates by current pollutant loads.

Estimated high reduction rates suggest that water pollution is very severe in this study area, and pollutant loads must be reduced within total allowable loads by continuous and long-term management.

ACKNOWLEDGEMENTS

This research was partly supported by the Korea Inter-University Institute of Ocean Science, Pukyong National University.

REFERENCES

[1] Baca, R. G. and Arnett, R. C., 1976, A limnological model for eutrophic lakes and impoundments, Battelee, Inc., Pacific northwest laboratories, Richland, Washington.

[2] Bowie, G. L., Pagenhopf, J. R., Rupp, G. L., Johnson, K. M., Chan, W. H., Gherini, S. A., Mills, W. B., Porcella, D. B. and Campbell, C. L., 1985, Rates, Constants, and Kinetics Formulations in Surface Water Quality Modeling, 2nd ed., EPA/600/3-85/040, USEPA, Athens, GA.

[3] Cerco, C. F., 1995, "Response of Chesapeake Bay to Nutrient Load Reductions", Journal of Environmental Engineering, Vol. 121, 549-557.

[4] Cerco, C. F. and Cole, T., 1993, "Three-Dimensional Eutrophication Model of Chesapeake Bay", Journal of Environmental Engineering, Vol. 119, 1006-1025.

[5] Di Toro, D. M., O'Connor, D. J. and Thomann, R. V., 1971, A dynamic model of the phytoplankton population in the Sacramento-San Joaquin Delta, In: Nonequilibrium systems in natural water chemistry, Advances in Chemistry Series, 106, American Chemical Society, Washington, D.C., 131-180.

[6] Drago, M., Cescon, B. and Iovenitti, L., 2001, "A three-dimensional numerical model for eutrophication and pollutant transport", Ecological Modelling, Vol. 145, 17-34.

[7] Hwang, H. M., Oh, J. R., Kahng, S. H. and Lee, K. W., 1999, "Tributyltin compounds in mussels, oysters and sediments of Chinhae Bay, Korea", Marine Environmental Research, Vol. 47, 61-70.

[8] Ishikawa, M. and Nishimura, H., 1983, "A new method of evaluating the mineralization of particulate and dissolved photoassimilated organic matter", Journal of Oceanographic Society of Japan, Vol. 39, 29-42 (in Japanese).

[9] Jorgensen, S. E., 1979, Handbook of Environmental Data and Ecological Parameters, International Society for Ecological Modeling.

[10] Karageorgis, A. P., Nikolaidis, N. P., Karamanos, H. and Skoulikidis, N., 2003, "Water and sediment quality assessment of the Axios River and its coastal environment", Continental Shelf Research, Vol. 23, 1929-1944.

[11] KORDI (Korea Ocean Research and Development Institute), 1995, A study on coastal zone utilization and integrated management (1), Ministry of Science and Technology, Korea, 865 pp. (in Korean).

[12] Kremer, J. N. and Nixon, S. W., 1978, A coastal marine ecosystem, In: Simulation and Analysis, Ecological Studies, 24, Springer-Verlag, Berlin, 217 pp.

[13] Lee, D. I., 2000, The numerical simulation on variation of phytoplankton maximum region in the estuary of Nakdong river, Ph.D. dissertation, Department of Environmental Engineering, Pukyong National University, 131 pp. (in Korean).

[14] Lee, D. I. and Park, C. K., 2002, "The modelling of winter water quality in the estuary of the Nakdong river", Journal of Korea Society on Water Quality, Vol. 18, 349-360 (in Korean).

[15] Lee, D. I., Park, C. K., and Cho, H. S., 2005, "Ecological modeling for water quality management of Kwangyang Bay, Korea", Journal of Environmental management, Vol. 74, 327-337.

[16] Lee, J. H., 1998, "Policy issues and management framework of Chinhae Bay, Republic of Korea", Ocean & Coastal Management, Vol. 38, 161-178.

[17] Lung, W. S., 1988, "The role of estuarine modeling in nutrient control", Water Science and Technology, Vol. 20, 243-252.

[18] Mark, D. J. and Bunch, B. W., 1992, Hydrodynamic and water quality modeling of Lower Green Bay, Estuarine and coastal modeling, In: proceeding of the 2nd international conference, ASCE, 657-668.

[19] MOE (Ministry of Environment), 1991, Report on the state of pollution in Chinhae Bay, MOE, Seoul, Korea, 502 pp. (in Korean).

[20] MOMAF (Ministry of Marine Affairs and Fixheries), 2002, Establishment of Action Plans for Coastal Environmental Management Areas, MOMAF, Seoul, Korea, 658 pp. (in Korean).

[21] Nakata, K., Horiguchi, F., Taguchi, K. and Setoguchi, Y., 1983, "Three dimensional tidal current simulation in Oppa Bay", Bulletin of the National Research Institute for Pollution and Resources, Vol. 12, 17-36 (in Japanese).

[22] Nakata, K., Ishikawa, K., and Matukawa, Y., 1985, "Numerical Models of Coastal Current and Transport in the Bay", Bulletin on Coastal Oceanography, Vol. 22, 96-108 (in Japanese).

[23] Nakata, K. and Taguchi, K., 1982, "Numerical simulation of eutrophication process in coastal bay by eco-hydrodynamic model, (2) Ecological modeling", Bulletin of the National Research Institute for Pollution and Resources, Vol. 12, 17-36 (in Japanese).

[24] National Academy of Science, 1972, A report of the committee on water quality criteria, Washington, DC.

[25] NFRDI (National Fisheries Research and Development Institute), 1997, Recent Red Tides in Korean Costal Waters, NFRDI, Busan, Korea (in Korean).

[26] O'Connor, D. J., Di Toto, D. M. and Thomann, R. V., 1975, Phytoplankton models and eutrophication problems, In: Ecological modeling in a resource management framework, C.S. Russell (ed.), Resources for the Future, Inc., Washington, D.C.

[27] Ogura, N., 1975, "Futher studies on decomposition of dissolved organic matter in coastal seawater", Marine Biology, Vol. 31, 101-111.

[28] Scavia, D. and Eadie, B. J., 1976, "The use of measurable coefficients in process formulations-zooplankton grazing", Ecological Modelling, Vol. 2, 315-319.

[29] Taguchi, K., and Nakata, K., 1998, "Analysis of water quality in Lake Hamana using a coupled physical and biochemical model", Journal of Marine Systems, Vol. 16, 107-132.

[30] Takeoka, H. and Murao, H., 1997, "Response of Water Quality to the Reduction of Nitrogen or Phosphorus Load from the Land", Bulletin on Coastal Oceanography, Vol. 34, 183-190 (in Japanese).

[31] Takeshi, H., 1988, "The role of modelling in the control of seawater pollution", Water Science and Technology, Vol. 20, 277-286.

[32] USEPA, 1997, Technical guidance manual for developing total maximum loads.

[33] Yanagi, T., Inoue, K., Montani, S. and Yamada, M., 1997, "Ecological modeling as a tool for coastal zone management in Dokai Bay, Japan", Journal of Marine Systems, Vol. 13, 123-136.

2006년 8월 21일 원고접수
2007년 1월 22일 수정본 채택